Supplementary material

Optimized CTAB-Modified Nanofibrillated Cellulose for Phosphate Recovery: Adsorption Mechanisms and Performance Insights

Archana Pandey[1], Yogesh Chandra Sharma[1], Ajay Kalamdhad[2]
[1]Indian Institute of Technology BHU, Varanasi, INDIA
[2]Indian Institute of technology Guwahati, Civil Engineering, Guwahati, INDIA
E-mail- archanapandey.rs.chy21@itbhu.ac.in

1. Methods

For preliminary screening, i.e., to evaluate the effect of CTAB concentration on phosphate adsorption, experiments were conducted in 100 mL glass bottles. Each bottle contained 0.1 g of series of adsorbents (with different molar concentration) added to 50 mL of 50 mg P/L solution at pH 7. The mixtures were agitated for 2 hours at a speed of 120 rpm. A blank phosphate solution without CTAB@NFC was used to confirm that the glass bottle had negligible adsorption. Filtration of the adsorbents was accomplished by a 0.45 µm nylon membrane syringe filter. The optimizing parameters included effect of CTAB concentration on phosphate adsorption, adsorption isotherms, kinetics, effects of solution pH, effect of competing anions and adsorbent dose.

The adsorption isotherms for phosphate were carried out with initial concentrations ranging from 5 to 40 mg/L (typical levels found in wastewater [1]. The adsorption kinetics experiment was performed at different time intervals (30, 60, 90, 120, 150, 180, 210, and 240 min) to determine the equilibrium concentration. The effect of solution pH on phosphate removal was examined across a pH range of 3.0 to 11.0, adjusted using appropriate amounts of either HCl or NaOH solutions (0.1 M). To study the effect of coexisting anions, Cl^-, F^-, NO_3^-, and HCO_3^- were added to the solution at different molar ratios to phosphate. For this investigation, concentrations reflecting typical levels in wastewater were utilized: 50 mg/L Cl^- (NaCl, 1.4 mM/L), 15 mg/L NO^{3-}

($NaNO_3$, 0.24 mM/L), 80 mg/L HCO_3^- ($NaHCO_3$, 1.3 mM/L), and 20 mg/L F^- (NaF, 0.47 mM/L). The ratio of adsorbent to initial adsorbate ions solution remained constant with that used in the kinetics/isotherm experiment. The influence of different concentration of adsorbent dosage (0.5- 2.5 g/L) was also performed to analyse the efficiency of the adsorbent. Finally, the phosphate laden CTAB@NFC was filtered, rinsed with deionized water, and dried in an oven at 65°C and labelled as CTAB@NFC* for future understanding. The dried adsorbent was then added to a 100 mL beaker, followed by the addition of 50 mL of deionized water. The mixture was stirred at 150 rpm for 24 h at pH 7. The concentrations of phosphate in the solution were then determined. This desorption experiment was repeated three times to analyse the retention capacity of CTAB@NFC for phosphate. All the experiments were conducted at 25 ± 2 °C.

1.1. Adsorption kinetics

The pseudo-first-order, pseudo-second-order and Elovich kinetic models were employed to predict the adsorption kinetics. The best-fit model was selected based on the correlation coefficient (R^2) value for regression.

1.2. Adsorption isotherm

Three isotherm models were used for the evaluation of the phosphate adsorption capacity namely Langmuir, Freundlich, and Sips isotherm models. All three isotherm models were adopted to ft the experimental data.

The equations of kinetic and isotherm models are provided in table S1:

Table 1. Kinetic and isotherm equations [2–4]**.**

Models	Equation	Parameters
Kinetic models		
Pseudo-first-order (PFO)	$q_t = q_e(1 - e^{-K_1 t})$	q_t $(mg\ P \cdot g^{-1})$is the adsorbed amount of phosphate at time t;
Pseudo-second-order (PSO)	$q_t = \frac{q_e^2 K_2 t}{1 + q_e K_2 t}$	q_e $(mg\ P \cdot g^{-1})$ is the adsorbed amount of phosphate at equilibrium;
Elovich	$q_t = \frac{1}{\beta}\ln(1 + \alpha\beta t)$	K_1 (min^{-1}), K_2 $(mg \cdot g^{-1} \cdot min^{-1})$, and $K_e(g \cdot min^{-0.5} \cdot g^{-1})$ are the rate constants of Pseudo-first-order, Pseudo-second-order, and Elovich, respectively;
		α $(mg \cdot g^{-1} \cdot h^{-1})$ is the initial adsorption rate, and β $(g \cdot mg^{-1})$ is the desorption constant.
Isotherm models		
Langmuir	$q_e = \frac{q_m K_L C_e}{1 + K_L C_e}$	q_e $(mg\ P \cdot g^{-1})$ is the adsorbed amount of phosphate at equilibrium;
Freundlich	$q_e = K_F C_e^{1/n_F}$	q_m $(mg\ P \cdot g^{-1})$ is the maximum adsorption capacity of adsorbent;
Sips	$q_e = \frac{q_m K_S C_e^{n_S}}{1 + K_S C_e^{n_S}}$	C_e $(mg\ P \cdot L^{-1})$ is the concentration of phosphate at equilibrium;
		K_L $(L \cdot mg^{-1})$, K_F $(mg \cdot g^{-1})$, K_S $(L^{n_s} \cdot mg^{-n_s})$ and K_T $(L \cdot g^{-1})$ are the adsorption constants of Langmuir, Freundlich, and Sips models, respectively;
		n_F n is heterogeneity factor (dimensionless);
		n_S is the heterogeneity factor that indicates the deviation from Langmuir isotherm (when n=1, the Sips equation reduces to the Langmuir isotherm).
		R (8.314 $J \cdot mol^{-1} \cdot K$), T (298.15 K) are the universal gas constant and experimental temperature, respectively.

2. Results and discussions

2.1. SEM-EDX data

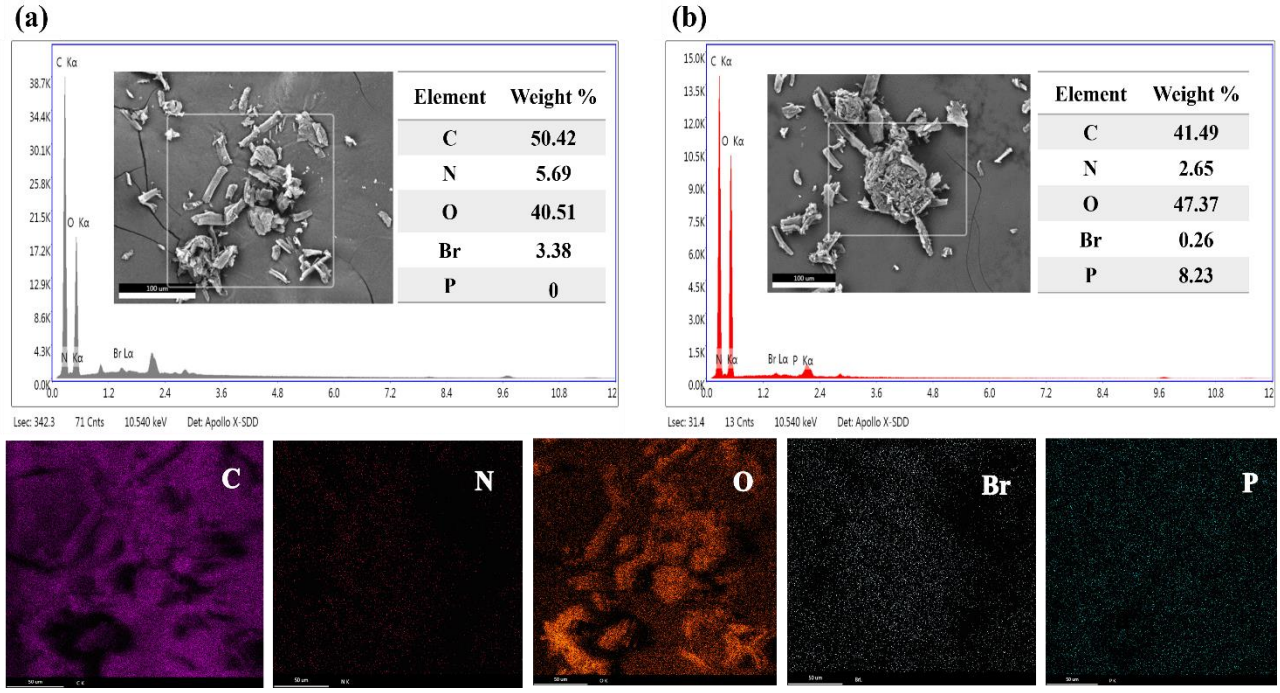

Fig. 1. EDS spectra and corresponding element distribution content of; **(a & b)** CTAB@NFC (before and after adsorption) respectively; EDS mapping of C, O, N, Br, P and elemental distribution of CTAB@NFC (after adsorption).

2.2. Effect of CTAB concentration on phosphate adsorption (pre-screen adsorption studies)

The preliminary assessment compared all the adsorbents to determine the optimal CTAB concentration for maximum phosphate adsorption (fig. 6a). Additionally, for each pre-screening adsorption test, parallel experiments using pristine NFC and CTAB were also measured to contrast their adsorption efficiencies. The experiments revealed that the removal percentage for both pristine NFC and CTAB was significantly lower across all tested phosphate concentrations. NFC showed a removal efficiency of 28.5%, likely attributed to repulsion resulting from the negative charge of NFC surface [5]. In contrast, CTAB demonstrated a removal efficiency of only 16.2%, likely due to nonspecific interactions between CTA^+ (cetyltrimethylammonium) cations and phosphate anions driven by electrostatic attraction (fig. 6a). The effect of

concentration of CTAB for modification of NFC significantly influences the sorption of anions including phosphate. The figure illustrates the phosphate removal percentage and equilibrium adsorption capacities of NFCs quaternized with varying molar concentration of CTAB. Increasing the molar concentration of CTAB from 0.5 mM to 1 mM corresponded to an increase in phosphate removal percentage up to 85% and an adsorption capacity of 21.7 mg/g. Beyond this threshold, the adsorption capacity of the adsorbent remained relatively stable despite increasing the molar concentration of CTAB. This behaviour is ascribed to alterations in the gross surface charge density of modified NFCs.

When 0.5 mM of CTAB is introduced to the NFC suspension, CTA^+ cations adhere onto the surface of NFCs, accompanied by their cationic headgroups orienting towards the particles, as illustrated in fig. 5 (i). This change is driven by the electrostatic attraction between the positively charged headgroups of the CTA^+ cations and the negatively charged OH^- groups on the NFC particle surface [6]. Consequently, the overall surface charge of the adsorbent ($CTAB_{0.5}$@NFC) becomes neutral, resulting in moderate adsorption capacity. Further increasing the CTAB concentration triggers the formation of admicelles on NFC surface (fig. 5 (ii)), due to hydrophobic interaction between the hydrophobic tails of both bound and free surfactant molecules [7]. As a result, reversal of surface charge takes place, and the adsorbent ($CTAB_{1.0}$@NFC) acquires positive charge. This attributes to increase in adsorption capacity of $CTAB_{1.0}$@NFC as demonstrated in fig. 6a. However, at concentration slightly above the critical micelle concentration (CMC) of CTAB (1 mM), the NFC surface saturates with surfactant molecules, and supplemental addition of surfactant induces the formation of free micelles above the critical concentration [8] (fig. 5 (iii)) and fails to contribute to alter the overall surface charge of the material. This can be evidenced by

the plateau observed in removal percentage of phosphate beyond CTAB CMC (≥ 1mM) (fig. 6a). Based on these results, all subsequent experiments are conducted using $CTAB_{1.0}$@NFC as adsorbent.

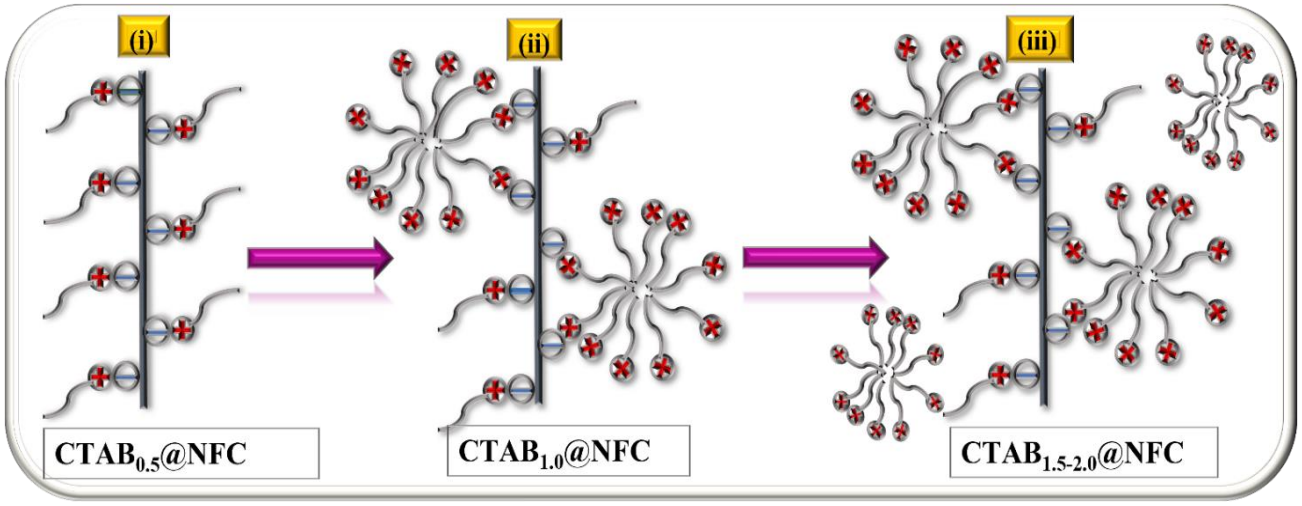

Fig. 2. Schematic illustration of the interactions between CTAB and NFC at varying molar concentrations (0.5, 1, 1.5 and 2 mM).

2.3. BET data

Table 2. BET specific surface area, average pore diameter, and total pore volume of synthesized CTAB@NFC

Parameters	Results
Specific surface area (m^2/g)	60.213
Average pore diameter (nm)	18.723
Total pore volume (cc/g)	0.09204

2.4. Adsorption kinetics data

Table 3. Adsorption kinetic parameters of phosphate removal on CTAB@NFC.

Models	Parameters	CTAB@NFC
Pseudo-first-order kinetic model	q_e (mg/g)	20.48
	K_1 (1/min)	0.043
	R^2	0.967

Pseudo-second-order kinetic model	q_e (mg/g)	22.66
	K_2 (g/mg/min)	0.028
	R^2	0.996
Elovich model	α (mg/g/min)	2.16
	β (g/mg)	0.20
	R^2	0.927

2.5. Adsorption isotherm data

Table 4. Adsorption isotherm parameters of phosphate removal on CTAB@NFC.

Models	Parameters	CTAB@NFC
Langmuir	q_m	52.004
	K_L	0.031
	R^2	0.978
Freundlich	n_F	1.405
	K_F	2.28
	R^2	0.966
Sips	q_m	30.35
	K_S	0.023
	n_S	1.21
	R^2	0.989

3. Plausible mechanism for phosphate removal

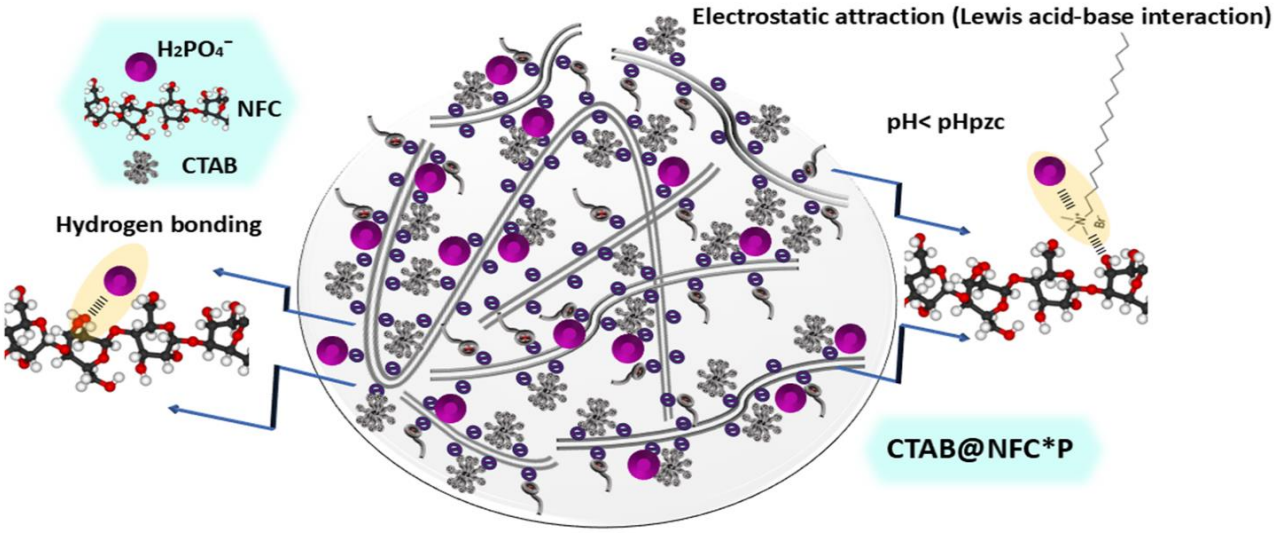

Fig. 3. Representation of adsorption mechanisms for phosphate removal on CTAB@NFC.

References

[1] H. Kong, W. Wang, J. Wang, G. Zhang, F. Shen, H. Jiang, Q. Li, Z. Huang, New insights into Lanthanum-Calcium bimetal for phosphate removal: Performance, molecular dynamics and life cycle assessment, Sep. Purif. Technol. 351 (2024) 128038. https://doi.org/10.1016/j.seppur.2024.128038.

[2] D.O. Omokpariola, Experimental Modelling Studies on the removal of crystal violet, methylene blue and malachite green dyes using Theobroma cacao (Cocoa Pod Powder)., SSRN Electron. J. (2022). https://doi.org/10.2139/ssrn.4235196.

[3] O.P. Murphy, M. Vashishtha, P. Palanisamy, K.V. Kumar, A Review on the Adsorption Isotherms and Design Calculations for the Optimization of Adsorbent Mass and Contact Time, ACS Omega 8 (2023) 17407–17430. https://doi.org/10.1021/acsomega.2c08155.

[4] K.Y. Foo, B.H. Hameed, Insights into the modeling of adsorption isotherm systems, Chem. Eng. J. 156 (2010) 2–10. https://doi.org/10.1016/j.cej.2009.09.013.

[5] H. Sehaqui, A. Mautner, U. Perez De Larraya, N. Pfenninger, P. Tingaut, T. Zimmermann, Cationic cellulose nanofibers from waste pulp residues and their nitrate, fluoride, sulphate and phosphate adsorption properties, Carbohydr. Polym. 135 (2016) 334–340. https://doi.org/10.1016/j.carbpol.2015.08.091.

[6] D. Ranjbar, M. Raeiszadeh, L. Lewis, M.J. MacLachlan, S.G. Hatzikiriakos, Adsorptive removal of Congo red by surfactant modified cellulose nanocrystals: a kinetic, equilibrium, and mechanistic investigation, Cellulose 27 (2020) 3211–3232. https://doi.org/10.1007/s10570-020-03021-z.

[7] B.L. Tardy, S. Yokota, M. Ago, W. Xiang, T. Kondo, R. Bordes, O.J. Rojas, Nanocellulose–surfactant interactions, Curr. Opin. Colloid Interface Sci. 29 (2017) 57–67. https://doi.org/10.1016/j.cocis.2017.02.004.

[8] M. Irfan, M. Usman, A. Mansha, N. Rasool, M. Ibrahim, U.A. Rana, M. Siddiq, M. Zia-Ul-Haq, H.Z.E. Jaafar, S.U.D. Khan, Thermodynamic and Spectroscopic Investigation of Interactions between Reactive Red 223 and Reactive Orange 122 Anionic Dyes and Cetyltrimethyl Ammonium Bromide (CTAB) Cationic Surfactant in Aqueous Solution, Sci. World J. 2014 (2014). https://doi.org/10.1155/2014/540975.